Atmos. Chem. Phys., 21, 16631–16644, 2021
https://doi.org/10.5194/acp-21-16631-2021

Atmospheric Chemistry and Physics
Open Access
EGU

Measurement report: Molecular characteristics of cloud water in southern China and insights into aqueous-phase processes from Fourier transform ion cyclotron resonance mass spectrometry

Wei Sun[1,2,3], Yuzhen Fu[1,2,3], Guohua Zhang[1,2,4], Yuxiang Yang[1,2,3], Feng Jiang[1,2,3,a], Xiufeng Lian[1,2,3,b], Bin Jiang[1,2], Yuhong Liao[1,2], Xinhui Bi[1,2,4], Duohong Chen[5], Jianmin Chen[6], Xinming Wang[1,2,4], Jie Ou[7], Ping'an Peng[1,2,4], and Guoying Sheng[1]

[1]State Key Laboratory of Organic Geochemistry and Guangdong Key Laboratory of Environmental Protection and Resources Utilization, Guangzhou Institute of Geochemistry, Chinese Academy of Sciences, Guangzhou 510640, PR China
[2]CAS Center for Excellence in Deep Earth Science, Guangzhou 510640, PR China
[3]University of Chinese Academy of Sciences, Beijing 100049, PR China
[4]Guangdong–Hong Kong–Macao Joint Laboratory for Environmental Pollution and Control, Guangzhou Institute of Geochemistry, Chinese Academy of Sciences, Guangzhou 510640, PR China
[5]State Environmental Protection Key Laboratory of Regional Air Quality Monitoring, Guangdong Environmental Monitoring Center, Guangzhou 510308, PR China
[6]Shanghai Key Laboratory of Atmospheric Particle Pollution and Prevention, Department of Environmental Science and Engineering, Fudan University, Shanghai 200433, PR China
[7]Shaoguan Environmental Monitoring Center, Shaoguan 512026, PR China
[a]now at: Institute of Meteorology and Climate Research, Karlsruhe Institute of Technology, Eggenstein-Leopoldshafen 76344, Germany
[b]now at: Institute of Mass Spectrometry and Atmospheric Environment, Guangdong Provincial Engineering Research Center for On-line Source Apportionment System of Air Pollution, Jinan University, Guangzhou 510632, PR China

Correspondence: Xinhui Bi (bixh@gig.ac.cn)

Received: 24 July 2021 – Discussion started: 23 August 2021
Revised: 8 October 2021 – Accepted: 17 October 2021 – Published: 15 November 2021

Abstract. Characterizing the molecular composition of cloud water could provide unique insights into aqueous chemistry. Field measurements were conducted at Mt. Tianjing in southern China in May, 2018. There are thousands of formulas ($C_{5–30}H_{4–55}O_{1–15}N_{0–2}S_{0–2}$) identified in cloud water by Fourier transform ion cyclotron resonance mass spectrometry (FT-ICR MS). CHON formulas (formulas containing C, H, O, and N elements; the same is true for CHO and CHOS) represent the dominant component (43.6 %–65.3 % of relative abundance), followed by CHO (13.8 %–52.1%). S-containing formulas constitute ∼5 %–20 % of all assigned formulas. Cloud water has a relative-abundance-weighted average O/C of 0.45–0.56, and the double bond equivalent of 5.10–5.70. Most of the formulas (>85 %) are assigned as aliphatic and olefinic species. No statistical difference in the oxidation state is observed between cloud water and interstitial $PM_{2.5}$. CHON with aromatic structures are abundant in cloud water, suggesting their enhanced in-cloud formation. Other organics in cloud water are mainly from biomass burning and oxidation of biogenic volatile organic compounds. The cloud water contains more abundant CHON and CHOS at night, which are primarily contributed by $-N_2O_5$ function and organosulfates, demonstrating the enhanced formation in dark aqueous or multi-phase reactions. While more abundant CHO is observed during the daytime, likely due to the photochemical oxidation and photolysis of N- or S-containing formulas. The results provide an improved understanding of the in-cloud aqueous-phase reactions.

Published by Copernicus Publications on behalf of the European Geosciences Union.

1 Introduction

On average, approximately 70 % of the Earth is covered by clouds (Stubenrauch et al., 2013; Herrmann et al., 2015). Cloud water is an essential sink of organics (Herckes et al., 2013) and provides a medium for the aqueous-phase reactions of dissolved gases and aerosols (Blando and Turpin, 2000), which can substantially modify the characteristics of the organics (McNeill, 2015; Kim et al., 2019). Aqueous-phase secondary organic aerosol (aqSOA) forming in the in-cloud aqueous-phase processes significantly contributes to the total secondary organic aerosol (SOA), with a negative impact on the visibility, human health, and climate (Ge et al., 2012; Huang et al., 2018; Schurman et al., 2018; T. Li et al., 2020; Smith et al., 2014; Paglione et al., 2020; Hallquist et al., 2009). Therefore, understanding the molecular characteristics and aqueous-phase reactions in cloud droplets is crucial to assessing their impact accurately.

Organics in cloud water mainly include organic acids (e.g., formic, acetic, oxalic acids, and other short-chain mono- and dicarboxylic acids; Sun et al., 2016), carbonyls (e.g., formaldehyde, acetaldehyde, glyoxal, and methylglyoxal; Ervens et al., 2013; van Pinxteren et al., 2016), as well as some heteroatom-containing compounds such as amino acids (Bianco et al., 2016b), organonitrates, and organosulfates (Zhao et al., 2013). Some less polar organics, such as n-alkanes (Herckes et al., 2002), benzene, toluene, ethylbenzene, and xylenes (Wang et al., 2020), polycyclic aromatic hydrocarbons (Herckes et al., 2002; Ehrenhauser et al., 2012), phenols, and nitrophenols (Lüttke et al., 1997, 1999) are also observed, though with a much lower fraction of dissolved organic materials (usually <1 %). The organics characterized using chromatographic and spectroscopic techniques only take a proportion of $\sim$ 20 % of all kinds of organics in cloud water (Herckes et al., 2013; Bianco et al., 2018). Ultra-high-resolution mass spectrometry, such as Fourier transform ion cyclotron resonance mass spectrometry (FT-ICR MS) has made it possible to characterize individual molecular formulas in complex mixtures, although the selectivity of detection still exists (Cho et al., 2015; Hockaday et al., 2009). In studies using ultra-high-resolution MS to characterize cloud or fog water, formulas were mainly divided into CHO, CHON, CHOS, and CHONS, based on the elemental composition, in which CHO and CHON were usually dominant (Zhao et al., 2013; Cook et al., 2017; Brege et al., 2018; Bianco et al., 2018, 2019). Boone et al. (2015) observed a high fraction of N-containing formulas in cloud water, compared with particles, and attributed it to the aqueous-phase formation. However, a more recent study carried out in Po Valley observed more CHO formulas in cloud water, while particle samples contained more N- and S-containing formulas. The authors attributed it to the high possibility of reactions with sulfate and nitrate ions in the concentrated environment of aerosol liquid water (Brege et al., 2018). Thus, more observations are needed to provide more convincing evidence of in-cloud aqueous-phase reactions.

Aqueous-phase reactions have been identified as being an important source of organics in cloud water in addition to the gas–liquid and particle–liquid partition. Aqueous-phase reactions mainly include radical and non-radical reactions. Under irradiation, hydroxyl radical ($OH\bullet$) is the primary radical in the atmosphere (Herrmann et al., 2010). In cloud water, the oxidation of precursors can be initiated by the hydrogen abstraction or electron transfer reaction driven by the $OH\bullet$, resulting in the formation of organic acids and condensed compounds (McNeill, 2015). On the one hand, photolysis causes the fragmentation of high-molecular-weight organic compounds, resulting in the formation of relatively low-molecular-weight compounds such as small acids, including oxalic, glyoxylic, and, in large quantities, formic and acetic acid (Renard et al., 2015; Schurman et al., 2018; Huang et al., 2018; Sun et al., 2010; Li et al., 2014; Löflund et al., 2002; Ye et al., 2020). These compounds are highly oxygenated owing to cloud processing (Brege et al., 2018; Sareen et al., 2016), as indicated by the fact that aqSOA has a higher O/C ratio ($\sim$ 1) than gas-phase SOA (0.3–0.5) in the atmosphere (Ervens et al., 2011). On the other hand, photochemistry also leads to the oligomerization of organics, such as pyruvic acid, phenols, and methyl vinyl ketone, under conditions relevant to deliquesced aerosols (Reed Harris et al., 2014; Renard et al., 2015; Yu et al., 2016). The oligomerization of tryptophan was also observed in synthetic cloud water (Bianco et al., 2016a). For the N- and S-containing organics, photochemistry may cause the release of inorganic nitrate and sulfate (Braman et al., 2020; Laskin et al., 2015; Brüggemann et al., 2020). The main radical in the atmosphere at night is $NO_3\bullet$, which can form from the gas-phase reaction between NO_2 and O_3 and then enter cloud droplets. The reactions between $NO_3\bullet$ and organics lead to the oxidation of organics or the addition of functional groups containing N atoms when the aqueous phase is concentrated and acidic (Herrmann et al., 2015; McNeill, 2015; Wang et al., 2008; Szmigielski, 2016; Rudziński and Szmigielski, 2019). Meanwhile, the radical nitration is believed to form dinitroaromatics in the aqueous phase (Kroflic et al., 2015). Non-radical reactions also lead to the formation of N-containing organics. Carbonyls can react with ammonium and amine without illumination, resulting in the generation of imidazoles and N-containing oligomers, especially in aerosol liquid water and evaporating cloud water (De Haan et al., 2009, 2011, 2018; Kua et al., 2011). In addition, the nucleophilic addition of nitrate to the isoprene-derived epoxydiol can effectively form organonitrates (Darer et al., 2011). While organosulfates can form through heterogeneous and bulk-particle-phase reactions (Brüggemann et al., 2020). Several formation mechanisms of organosulfates, such as the acid-catalyzed ring opening of epoxides, sulfate esterification, nucleophilic substitution of alcohols with sulfuric acid, and sulfoxy radical reactions, have been proposed in recent years (Brüggemann et al., 2020). The non-

radical reactions in the aqueous phase also include hydrolysis, hydration, the Fenton reaction, translation metals reactivity with organics, probably ozone reactivity at the gas or liquid interface, and so on (McNeill, 2015; Deguillaume et al., 2005; Herrmann et al., 2015).

To date, only a few studies have reported on the molecular characteristics of cloud water using ultra-high-resolution MS, hampering our understanding of aqueous-phase reactions on the composition of cloud water. In this study, cloud water and $PM_{2.5}$ samples at a remote mountain site were collected and analyzed by FT-ICR MS. The primary objectives of this study are to investigate the molecular characteristics and composition of the organics in cloud water and to explore the potential influences of aqueous-phase reactions.

2 Materials and methods

2.1 Sample collection and pretreatment

A sampling campaign was carried out at an atmospheric monitoring station (112°53′56″ E, 24°41′56″ N; 1690 m a.s.l. – above sea level) located at the Tianjing Mountain in southern China (Fig. S1 in the Supplement). The site is located in a natural conservation zone far away from anthropogenic activities, which is affected mainly by local biogenic emissions and long-distance transport during the monsoon seasons.

A Caltech Active Strand Cloud water Collector, version 2 (CASCC2), was used for cloud water collection (Demoz et al., 1996). Cloud events were identified using the humidity sensor and the visibility meter in a co-working ground-based counterflow virtual impactor (model 1205; Brechtel Manufacturing Inc, USA) according to the following criteria: visibility ≤ 3 km, relative humidity ≥ 95 %, and no precipitation. During sampling, cloud droplets entered the collector, powered by a rear fan, and condensed on a bank of Teflon strands at a flow rate of 5.8 m^3 min^{-1} and a collection efficiency of 86 %. Condensed cloud water flowed into the pre-cleaned sample jar through a Teflon tube equipped at the bottom of the collector. The pH of the cloud water was measured using a pH meter. Samples were refrigerated immediately after sampling and kept until the analysis. The cloud liquid water content (LWC) during the sampling was calculated as follows (Guo et al., 2012):

$$\mathrm{LWC} = \Delta m/(\Delta t \times \eta \times Q),$$

where Δm represents the mass of the sample (g), and Δt represents the sampling interval (minutes). η is the collection efficiency, which is regarded as 86 % for cloud droplets larger than 3.5 µm, and Q is the airflow of the CASCC2, i.e., 5.8 m^3 min^{-1}. A total of 24 cloud water samples (sample ID: CL1-24) were collected in succession during a long-duration cloud event that lasted from 8 to 13 May 2018. To investigate the molecular characteristics of the organics and the effects of aqueous-phase processes, six samples collected from 11 to 12 May (CL12-17; Table 1) were selected for FT-ICR MS analysis in detail since these six samples were all collected during the maintenance stage of a cloud event with stable pH and LWC (Table 1), stable meteorological conditions, and no dramatic change in air masses origin (Figs. S1, S2). The sampling interval of six samples is presented in Table 1 and Fig. S2. The samples CL12, CL13, and CL14 were collected during the daytime of 11 May, while the other three samples (CL15, CL16, and CL17) could be roughly regarded as nighttime samples, although CL15 was partly collected before sunset.

Table 1. The sampling interval, liquid water content (LWC; grams per cubic meter), and pH of each sample.

Time	Sample ID	Sampling interval	LWC	pH
Daytime	CL12	2018/5/11 10:15–12:40	0.17	4.16
	CL13	2018/5/11 12:40–15:00	0.17	4.22
	CL14	2018/5/11 15:00–18:00	0.19	4.37
Nighttime	CL15	2018/5/11 18:00–21:00	0.17	4.28
	CL16	2018/5/11 21:00–24:00	0.16	4.18
	CL17	2018/5/12 00:00–08:15	0.12	4.13

Quartz fiber filters (Whatman plc, UK) were used to collect interstitial $PM_{2.5}$ samples at the same site. A $PM_{2.5}$ sampler (PM-PUF-300; Mingye Technology Co., Ltd., China) at a flow rate of 300 L min^{-1} was used for sampling. The sampling interval of $PM_{2.5}$ was roughly 24 h. In total, two samples of $PM_{2.5}$ were collected within 2 d (P1 from 11 May at 10:14 LT to 12 May at 09:48 LT; P2 from 12 May at 10:15 LT to 13 May at 10:15 LT) during the investigated cloud events. The samples were stored at −20°C immediately after sampling. For the laboratory analysis, 60 cm^2 of the sample filters were cut into pieces and soaked in ultra-clean water. Then the water-soluble organic matter in $PM_{2.5}$ was separated into the ultra-clean water by 30 min ultrasonic extraction three times; after that the extract was filtered using 0.22 µm polytetrafluoroethylene filters. The extract was then pretreated and analyzed used the same methods as with cloud water samples.

For FT-ICR MS analysis, water-soluble organic compounds in cloud water and $PM_{2.5}$ extracts were isolated using solid-phase extraction (SPE; Zhao et al., 2013; Bianco et al., 2018). The SPE cartridges (Strata-X; Phenomenex, USA) were preconditioned sequentially with 3 mL of isopropanol, 6 mL of acetonitrile, 6 mL of methanol containing 0.1 % of formic acid, and 6 mL of ultrapure water containing 0.1 % formic acid. Then, 40 mL of cloud water without pH adjustment and $PM_{2.5}$ extracts with pH adjusted to 4.5 using formic acid were added to the cartridge at a flow rate of approximately 1 mL min^{-1}. The inorganic salts were removed from the cartridge using 4 mL of ultrapure water containing 0.1 % formic acid. Note that some low-weight organic molecules are expected to be lost in this step. The cartridges were then freeze-dried, and the analytes were eluted using 3 mL of ace-

tonitrile, methanol, and ultrapure water (45/45/10; $v:v:v$) at pH 10.4, with the pH being adjusted using ammonium hydroxide. All the solvents were HPLC grade. Blank samples of the cloud water and $PM_{2.5}$ were processed and analyzed following the same procedure as the samples.

2.2 Instrumental analysis and data processing

A solariX XR FT-ICR MS instrument (Bruker Daltonics GmbH & Co. KG, Bremen, Germany) equipped with a 9.4 T refrigerated, actively shielded superconducting magnet (Bruker France S.A.S., Wissembourg, France) and a ParaCell analyzer cell was used for the analysis in this study. An electrospray ionization (ESI) source (Bruker Daltonics GmbH & Co. KG, Bremen, Germany) at the negative ion mode was used to ionize the organics. ESI is a soft ionization technique that offers minimal fragmentation of the analytes (Mazzoleni et al., 2010). $[M\text{-}H]^-$ was detected at the negative ion mode. The coupling of ESI and FT-ICR MS with ultra-high-mass resolution makes it possible to characterize the element constitution within molecules. Note that ESI is efficient at ionizing molecules having polar functional groups containing nitrogen and oxygen atoms (Cho et al., 2015). The direct infusion method was used in this study. The samples were redissolved in 1 mL of methanol and injected into an ESI source at a flow rate of 200 µL h^{-1}. A nebulizer gas pressure of 1 bar, a dry gas velocity of 4 L min^{-1} and temperature of 200 °C, and capillary voltages of +4500 V and the end plate offset −500 V were used for the ESI source. The optimized mass for quadrupole (Q1) was 170 Da. An argon-filled hexapole collision pool was operated at 2 MHz and 1400 Vpp (volts; peak to peak) RF (radio frequency) amplitude. The time of flight was 0.7 ms, the mass range was 150–800 Da, and the ion accumulation time was 0.1 s. A total of 128 continuous 4 mega-data FT-ICR transients were co-added to enhance the signal-to-noise ratio and dynamic range. A typical mass-resolving power ($m/\Delta m$ 50 %, where Δm50 % is the magnitude of the mass spectral peak full width at half-maximum peak height) of more than 450 000 at m/z 319 with <0.3 ppm (parts per million) absolute mass error was achieved. The mass spectra were calibrated externally using measurements of a known homologous series of N_1 and O_2 molecules (e.g., $C_{16}H_{31}O_2$, $C_{17}H_{33}O_2$, $C_{18}H_{35}O_2$, etc., that was only separated by $-CH_2$ units) frequently detected in a crude oil sample before sample detection. The final spectrum was internally recalibrated with typical class species peaks in cloud water samples ($-O_4$ species) using quadratic calibration in DataAnalysis 5.0 (Bruker Daltonics GmbH & Co. KG, Bremen, Germany; Jiang et al., 2019). All the mathematically possible formulas for all the ions with a signal-to-noise ratio greater than 10, considering a mass tolerance of ±0.6 ppm, were calculated. The maximum numbers of atoms for the formula calculator were set to 30 ^{12}C, 60 ^{1}H, 20 ^{16}O, 2 ^{14}N, 2 ^{32}S, 1 ^{13}C, 1 ^{18}O, and 1 ^{34}S. Formulas assigned to isotopomers (i.e., ^{13}C, ^{18}O, or ^{34}S) were not discussed in this study. Thus, the chemical formula $C_cH_hO_oN_nS_s$ was obtained. Future selecting was applied using the following criteria to exclude formulas not detected frequently in natural materials: O/C ≤ 1.2, 0.3 ≤ H/C ≤ 2.25, N/C ≤ 0.5, S/C ≤ 0.2, 2C + 2 > H, C + 2 > O, and obeying N rule. Finally, only intensities of sample ion peaks enhanced at least 100 times higher than those in the blank were retained for further data analysis in order to avoid possible contamination. The double bond equivalent (DBE) can be used to evaluate the number of rings and double bonds in a molecule (An et al., 2019). The DBE of each assigned molecular formula ($C_cH_hO_oN_nS_s$) was calculated as follows:

$$\mathrm{DBE} = (2c + 2 - h + n)/2.$$

The oxidation state of carbon atoms (OS_C) was calculated as follows, based on the approximation described in Kroll et al. (2011) and Brege et al. (2018):

$$\mathrm{OS_C} \approx 2 \times o/c - h/c - 5 \times n/c - 6 \times s/c. \quad (1)$$

The modified aromaticity index (AI_{mod}) was first proposed by Koch and Dittmar (2006) to evaluate the aromaticity of high-resolution mass data, as follows:

$$\mathrm{AI_{mod}} = (1 + c - 0.5 \times o - s - 0.5 \times h)/(c - 0.5 \times o - s - n).$$

$AI_{mod} \geq 0.5$ and 0.67 represent the existence of aromatic and condensed aromatic structures, respectively (Koch and Dittmar, 2006).

The relative abundance of each formula was represented by the intensities of each peak after normalization by the maximum intensity in each sample. Note that both the recovery of SPE and the selective ionization of negative ESI might cause a bias of mass spectra to certain peaks, and ESI FT-ICR MS is not a purely quantitative technique. So, the intensity of the peak for each formula is a product of its concentration and ionization efficiency. However, since all of the samples were pretreated using the same procedure and measured using the same instrumental conditions, each spectrum was biased in an equal fashion, so relative peak intensities within the acquired spectra can be compared to each other, although they cannot be related back to concentrations in the original samples (Sleighter et al., 2010; Wozniak et al., 2014). The relative-abundance-weighted average elemental ratios of oxygen, carbon, and hydrogen (i.e., O/C, H/C, etc.) and other characteristic parameters were calculated following Song et al. (2018):

$$\mathrm{O/C_w} = \Sigma(\mathrm{O/C_i} \times \mathrm{Int_i})/\Sigma\mathrm{Int_i} \quad (2)$$

$$\mathrm{H/C_w} = \Sigma(\mathrm{H/C_i} \times \mathrm{Int_i})/\Sigma\mathrm{Int_i} \quad (3)$$

$$\mathrm{DBE_w} = \Sigma(\mathrm{DBE_i} \times \mathrm{Int_i})/\Sigma\mathrm{Int_i} \quad (4)$$

$$\mathrm{OS_{Cw}} = \Sigma(\mathrm{OS_{Ci}} \times \mathrm{Int_i})/\Sigma\mathrm{Int_i}, \quad (5)$$

where Int_i represents the intensity of the mass spectrum for each individual molecular formula, i. The discussion in this

paper is based on the weighted average values unless otherwise specified; thus, the subscript w is omitted for brevity in the following texts.

Cloud water samples were also analyzed for ionic species. Descriptions of these analyses are available elsewhere (Guo et al., 2012; Bianco et al., 2018). Briefly, water-soluble inorganic ions and oxalate ($C_2O_4^{2-}$) were detected using an ion chromatograph (883 Basic IC plus; Metrohm AG, Switzerland) with suppressed conductivity detection and a Metrosep C 4 – 150/4.0 column (Metrohm AG, Switzerland) for cations and a Metrosep A Supp 5 – 150/4.0 column (Metrohm AG, Switzerland) for anions.

The 72 h back trajectories were displayed using the Hybrid Single-Particle Lagrangian Integrated Trajectory model (HYSPLIT; https://ready.arl.noaa.gov, last access: 11 November 2021) (Stein et al., 2015; Lin et al., 2017). The endpoint of the trajectory in the model was set to a height of 1800 m a.s.l. In addition, the meteorological conditions during sampling and water-soluble ions concentrations are provided and discussed in Text S1.

3 Results and discussion

3.1 Overview of molecular formulas of cloud water and comparison to the interstitial $PM_{2.5}$

A total of 1691, 1546, 1604, 1264, 2364, and 2767 molecular formulas were identified in CL12-17 samples, respectively. According to the elemental compositions, four groups (CHO, CHON, CHOS, and CHONS) were assigned. The reconstructed mass spectrum of a typical sample, CL12, is presented in Fig. 1a. The most intensive ion peaks are within the range of m/z 200–400. A similar pattern is also found in cloud (Zhao et al., 2013; Bianco et al., 2018; Cook et al., 2017), fog (Brege et al., 2018), and aerosols (Lin et al., 2012; Mazzoleni et al., 2012).

In cloud water, CHON is the most frequently observed group, representing more than 60 % of the total number of assigned formulas. CHO contributes to 16.3 %–28.3 % of the total number of identified formulas, while the proportions of S-containing formulas (CHOS and CHONS) are much lower (3.6 %–9.4 % and 3.7 %–9.3 %, respectively; Table S2). The relative abundance of each group is evaluated, as shown in Fig. 1b and Table S2. The relative abundance fraction (f_{RA}) of the CHON group is 43.6 %–65.3 % (54.9% on arithmetic average), and CHO contributes 13.8 %–52.1 % (34.7 % on arithmetic average). S-containing formulas constitute the remaining fraction, which is approximately 5 %–20 % (Table S2). The fractions of four groups in relative abundance and in number are different, which is mainly attributed to some formulas with high intensities contributing much more to relative abundance than to the number. Note that the abundant CHO and CHON cannot be directly related back to the composition of samples due to the preferential detection of these molecules in negative ESI. However, the comparison among the samples is still meaningful since they are expected to have the same bias.

The cloud water shows a distinct pattern of molecular composition with the interstitial $PM_{2.5}$. In two $PM_{2.5}$ samples, 1198 and 1057 formulas are identified in which CHO and CHON are dominant. The smaller number of assigned formulas in $PM_{2.5}$ may be mainly related to the low concentration of total organics in $PM_{2.5}$ extracts. The CHO group contributes to 39.9 %–49.8 %, while the CHON group contributes to 31.8 %–51.0 %. The S-containing formulas constitute the remaining fraction (9.1 %–18.4 %). Similar results can also be obtained by f_{RA} of CHO (44.0 %–55.5 %), CHON (24.3 %–47.3 %), and S-containing formulas (8.7 %–20.3 %; Table S3). At three sites in the Pearl River Delta (PRD), more than half of all detected formulas were assigned as CHO, while CHON only accounted for 8 %–19 % in the aerosols (Lin et al., 2012). The higher fraction of CHON in cloud water compared with $PM_{2.5}$ in the PRD and interstitial particles is consistent with the previous finding (Boone et al., 2015), likely indicating the formation of N-containing organics in cloud water.

3.2 Effects of cloud processing on oxidation metrics and aromaticity of the molecular formulas

3.2.1 Oxidation metrics

O/C and OS_C are employed to evaluate the oxidation degree of molecules in cloud water. In six cloud water samples, the average O/C values range from 0.45 to 0.56 (Table S4). No significant differences in O/C are observed between cloud water and $PM_{2.5}$, of which average O/C values are 0.45–0.56 (Table S5). In the Van Krevelen (VK) plot, CHON formulas distribute in a wide area (Figs. 2 and S3). Some of them, with O/C exceeding 0.8, distribute in the top-right corner of the plots, which also result in higher O/C of CHON on average (0.51–0.62; Table S4) compared with CHO, of which O/C ratios range from 0.34 to 0.46. On a relative-abundance-weighted average, the O/C ratios of CHOS and CHONS range from 0.36 to 0.51 and from 0.65 to 0.88, respectively. This is not unintelligible if we note that the N and S atoms in the CHON and S-containing formulas would probably combine with O (e.g., $-NO_2$, $-NO_3$, or $-SO_3$ function group), leading to the higher average O/C of non-CHO formulas. The OS_C value excludes the influence of oxygen atoms combined with H, N, and S; thus, it is a more applicative proxy to evaluate the oxidation state of carbon atoms. The average OS_C values range from -0.91 to -0.72 in cloud water (Table S4) and range -0.84 to -0.61 in $PM_{2.5}$ (Table S5). Being limited by the sampling size, no statistical difference of OS_C can be identified between cloud water and $PM_{2.5}$. However, a higher OS_C of detected formulas, especially CHO, appears in $PM_{2.5}$ samples (-0.40 in the P2 sample). A similar phenomenon is also observed in CHOS. This is not consis-

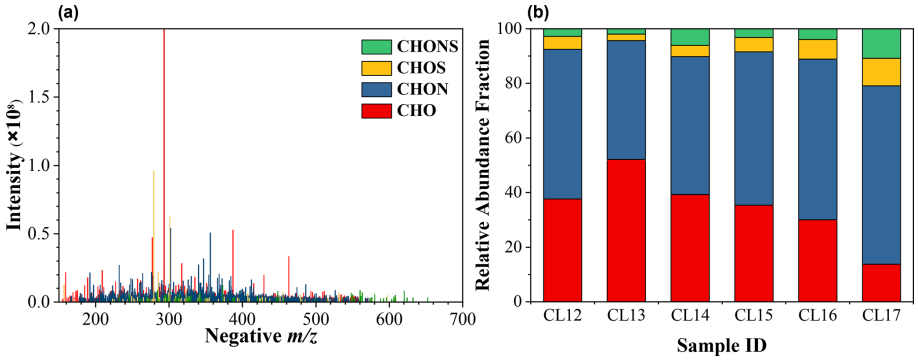

Figure 1. Reconstructed FT-ICR mass spectrum of a typical sample, namely CL12 **(a)**. Relative abundance fraction of the four groups (CHO, CHON, CHOS, and CHONS) in the six cloud water samples **(b)**.

tent with the current understanding that precursors and products in the aqueous phase have a higher O/C, which generally causes the high water-solubility of molecules (Ervens et al., 2011). However, a previous aircraft sampling also observed a lower O/C in cloud water than below-cloud atmospheric particles (Boone et al., 2015), suggesting that the effects of aqueous-phase reaction may be complex in the actual atmosphere. Previous studies using the large-eddy simulation model have shown that the in-cloud residence time of the parcel is on the scale of a few minutes (Stevens et al., 1996; Feingold et al., 1998); thus, some masses formed in cloud droplets may remain in aerosols via the evaporation of the droplets, resulting some high oxidation organics entering the interstitial $PM_{2.5}$. We cannot completely rule out the influence of cloud cycling; however, this impact may be limited because of the stable meteorological conditions with constant temperature, wind, and saturated or supersaturated water vapor during sampling (Fig. S2). We note that $PM_{2.5}$ samples were collected during the cloud event; high aerosol liquid water content in $PM_{2.5}$ likely provides a sink containing more concentrated precursors for the aqueous-phase reactions compared with cloud water. However, no formation mechanism of more oxidized organics in aerosol liquid water has been proposed in previous studies; thus, future research of aqueous-phase reactions in the atmosphere is needed. In four groups, CHO has the highest OS_C values ($-0.80 \sim -0.54$; Table S4), which may be related to the high abundance of carboxyl groups in CHO.

To investigate the diurnal variation in oxidation metrics in cloud water, daytime and nighttime samples are compared. The O/C ratios show no identified diurnal variation, except for the CHO group. The O/C ratios and OS_C of CHO collected during the daytime are slightly lower than the nighttime (Table S4). This is not consistent with the high oxidation capacity under the illumination during the daytime, indicating that the oxidation degree of the organics in cloud water is not exclusively affected by the illumination. The difference in the origin of air masses and the aging processes may also influence the cloud chemistry. However, since the database is limited, the further conclusion cannot be drawn based on them.

3.2.2 Aromaticity

The unsaturation and aromaticity of molecular formulas can be evaluated using the H/C ratios and the DBE, where low H/C and high DBE indicate a high degree of unsaturation, and, to some extent, aromatic structure. On a relative-abundance-weighted average, H/C ratios in cloud water range from 1.44 to 1.49, with no statistical difference when compared to $PM_{2.5}$ (1.40–1.53). In the VK plot, CHOS and CHONS occupy an upper area of the diagram with high H/C ratios (Fig. 2), indicating that they may have higher saturation compared with CHO and CHON. On a weighted average, DBE values in cloud water range from 5.10 to 5.70 (Table S4), which are generally higher than that in $PM_{2.5}$ (4.74–5.04; Table S5). The weighted average DBE values of CHO, CHON, CHOS, and CHONS are 4.96–6.12, 5.44–6.09, 2.72–4.58, and 3.01–4.29, respectively. DBE values are also projected onto the plots of DBE versus carbon atom numbers (Fig. 3). DBE values generally increase with carbon number, and CHOS and CHONS distribute in a range with low DBE values. The higher unsaturation degree of CHO and CHON is likely corresponding to the high abundance of aromatic functions.

Another commonly used metric of aromaticity is AI_{mod}. In cloud water, most of the formulas (91.1 %–98.3 % of CHO, 79.2 %–97.5 % of CHON, 93.5 %–98.8 % of CHOS, and 95.7 %–100.0 % of CHONS in f_{RA}) are assigned as aliphatic or olefinic molecules (Table S6). The f_{RA} of aliphatic and olefinic molecules in $PM_{2.5}$ also exceeds 90 %. The high fraction of aliphatic and olefinic and the low fraction of aromatic structures are also observed in aerosols at a remote site (An et al., 2019). However, it is quite different from the primary emissions, including biomass burning, coal combustion, and traffic emissions, of which the fraction of aromatic structures is higher (Song et al., 2018; Tang et al., 2020). The urban aerosols collected in Guangzhou, southern China,

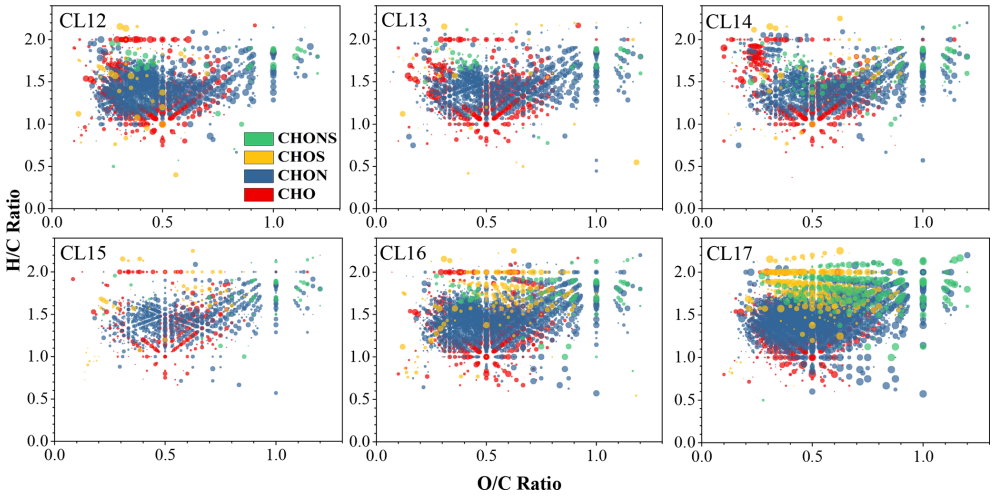

Figure 2. Van Krevelen diagrams as a function of four groups (CHO, CHNO, CHOS, and CHNOS) for the cloud water samples. The larger point in the diagram represents the higher relative abundance of the formula.

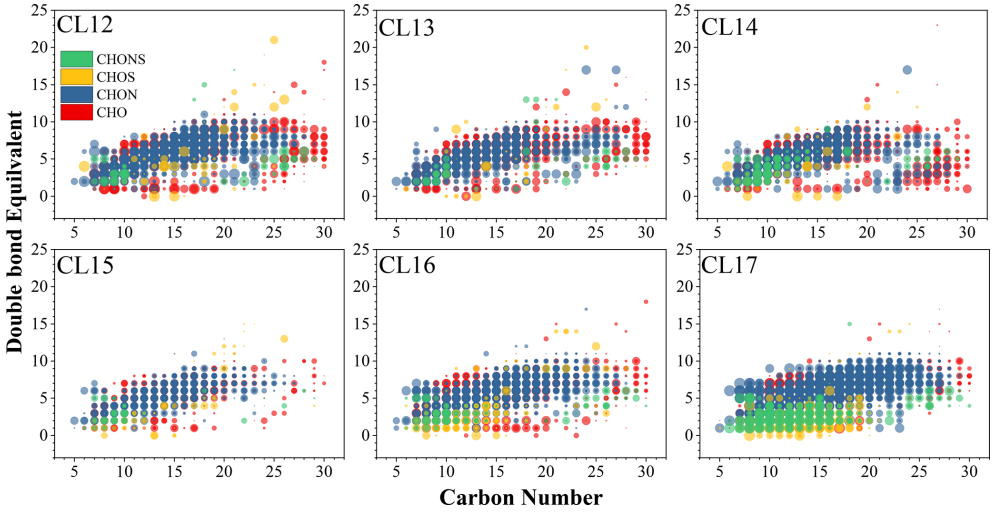

Figure 3. The double bond equivalent (DBE) versus the number of C atoms for unique molecular formulas in cloud water samples. The larger point in the diagram represents the higher relative abundance of the formula.

which may be mainly influenced by local primary emissions, also have a high fraction of aromatic molecules (>20 %; Zou et al., 2020), implying that the aging processes likely reduce the aromaticity of organics. In four groups of molecules in cloud water, CHON has the most (2.5 %–20.8 % in f_{RA}) aromatic structures, consistent with the high DBE values (unsaturation) of CHON. Previous studies conducted in the Po Valley, Italy (Brege et al., 2018) and Fresno, CA, USA (Leclair et al., 2012) also observed a higher fraction of aromatics in CHON than the S-containing groups in fog water. The aromatic species may provide the precursors of aqueous-phase reactions (Wang et al., 2021), while, in this study, the possible dinitrophenols in cloud water contribute to the high f_{RA} of aromatic structures in CHON significantly, which may be related to the aqueous-phase reactions (see the detailed discussion in Sect. 3.4).

3.3 Molecular composition of cloud water

3.3.1 CHON

In cloud water, CHON formulas show no prominent carbon number peaks, except for sample CL17 (Fig. S4), and one or two nitrogen atoms are assigned to them (Fig. 4). Both the N_1 and N_2 categories contain 1–14 oxygen atoms. The most abundant class of N_1 formulas is $-N_1O_8$ or $-N_1O_7$ (Fig. 4), which includes $C_{12}H_{17}NO_8$, $C_{15}H_{19}NO_8$, $C_{17}H_{27}NO_7$, $C_8H_{11}NO_7$, and so on. More than 77.7 % of the CHON formulas in f_{RA} in all six samples have O/N ratios

exceeding 3, indicating that the N atoms in these molecules may be in the $-NO_3$ functional group (Zhao et al., 2013). Samples CL12–16 show no prominent peak of the function classes in the N_2 category, but a dominant peak of the $-N_2O_5$ class is observed in CL17 (Fig. 4), where $C_8H_8N_2O_5$ and $C_7H_6N_2O_5$ are the two most abundant formulas. These formulas probably belong to dinitrophenols and their derivatives.

To evaluate the contribution of primary sources, we compared the molecular composition in cloud water to that in particles emitted from the primary sources such as biomass burning (including corn straw, pine branches, and rice straw) and coal combustion using the same analytical instrument (Song et al., 2018). In cloud water, 40.9 %–51.4 %, 21.9 %–27.1 %, and 48.1 %–59.4 % (in terms of number fraction) of CHON molecules appear in the smoke particles of corn straw, pine branches, and rice straw, indicating a non-negligible contribution from biomass burning, while only 7.7 %–10.5 % of CHON molecules in cloud water correspond to the coal combustion emission, suggesting its smaller contribution to the molecular composition of cloud water. Note that the comparison is only based on the molecular formulas given by FT-ICR MS, and the isomeride can not be distinguished; thus, the results only represent a possible relationship with the different sources. Additionally, some N-containing molecules were also detected in monoterpene SOA (Park et al., 2017; Zhang et al., 2018), in which the products such as $C_7H_{9,11}NO_{7\text{-}8}$, $C_8H_{11}NO_{7\text{-}8}$, $C_9H_{13,15}NO_{7\text{-}8}$, and $C_{10}H_{15,17,19}NO_{7\text{-}8}$ are detected in cloud water, indicating a contribution from monoterpene oxidation.

3.3.2 CHO

For CHO formulas in cloud water, a prominent C_{17} peak is observed in all six samples (Fig. S4), in which the most abundant formula is $C_{17}H_{26}O_4$, which also causes a significant peak of the O_4 class (Fig. 4). The formula may belong to a lipid-like molecule based on the classification in the VK plot (Bianco et al., 2018). Considering the intensive emission of biogenic volatile organic compounds (BVOCs) around the sampling site, the oxidation products of BVOCs may also contribute to the molecular composition. Putman et al. (2012) reported the molecular composition of α-pinene ozonolysis SOA using FT-ICR MS. Including the most abundant $C_{17}H_{26}O_4$, 24.0 %–39.1 % (in terms of the number fraction) of the CHO formulas in cloud water are corresponding to the yields of α-pinene ozonolysis. In addition, cloud water contains formulas that have been observed in the combustion of coal and biogenic materials. Specifically, 24.2 %–35.8 %, 65.9 %–77.3 %, 50.7 %–69.3 %, and 61.1 %–76.7 % of the CHO formulas in cloud water, by number, were detected in the smoke emitted from the combustion of coal, corn straw, pine branches, and rice straw, respectively (Song et al., 2018), indicating that combustion also potentially contributes to the CHO group in cloud water.

3.3.3 S-containing formulas

Most of the CHOS formulas in cloud water have C_{13} or C_{14} peaks (Fig. S4), and $-SO_3$ or $-SO_4$ represent the most abundant classes of CHOS (Fig. 4). We divided the CHOS formulas into the following two classes according to the O/S ratios: $CHOS_{O/S\geq4}$ and $CHOS_{O/S<4}$. When $O/S \geq 4$, CHOS can be provisionally identified as organosulfates (Lin et al., 2012). The O/S ratios of most of the CHOS formulas (78.9 %–95.8 % in number fraction and 87.5 %–98.6 % in f_{RA}) in cloud water exceed 4. $CHOS_{O/S<4}$ accounts for 1.4 %–12.5 % in f_{RA} of all the CHOS formulas in cloud water, indicating that reduced S groups exist in these formulas. Some of them are aliphatic-like, such as $C_{24}H_{42}O_3S$ and $C_{29}H_{52}O_3S$. Some are aromatic-like with high DBE values, such as $C_6H_6O_3S$, which may be an aromatic ring bearing a $-SO_3H$ group. Some of them may have more than one aromatic ring, such as $C_{17}H_{16}O_3S$ and $C_{20}H_{18}O_3S$. Note that the aromaticity of these formulas cannot be identified accurately using AI_{mod} values, since the value is a conservative method to evaluate the aromaticity (Koch and Dittmar, 2006). The presence of the aromatic structure in these molecules indicates that they are likely emitted by anthropogenic sources or biomass burning (Ervens et al., 2011). Most of the CHONS formulas clearly peak at C_{10} (Fig. S4) and have more than seven O atoms (Fig. 4), allowing the presence of both sulfate and nitrate functional groups. These species can be nitrooxy organosulfates, which have been widely observed in the cloud/fog water (Zhao et al., 2013; Brege et al., 2018) and aerosols (Wozniak et al., 2014). For the detected S-containing formulas in cloud water, 6.2 %–23.0 %, 15.9 %–33.6 %, and 15.0 %–34.3 % in terms of number fraction are corresponding to the molecules in particles emitted by burning of corn straw, pine branches, and rice straw, respectively, while 21.2 %–43.1 % (37.3 % on arithmetic average) are corresponding to that in coal combustion (Song et al., 2018), indicating that coal combustion contributes to S-containing formulas in cloud water more significantly compared to that with CHO and CHON.

3.4 Organic matter formed by in-cloud aqueous-phase reactions

3.4.1 Formation of dinitrophenols

To investigate the formation of molecules in cloud water, we compared the molecular formulas in cloud water with $PM_{2.5}$. For CHON, the $-N_1O_8$ or $-N_1O_7$ formulas are also abundant in $PM_{2.5}$ samples (Fig. S5), suggesting that these formulas may not only form in cloud water. However, the formulas with high intensities, e.g., $C_8H_8N_2O_5$, $C_7H_7N_2O_5$, and $C_6H_4N_2O_5$ in cloud water, are not detected in $PM_{2.5}$ samples. Earlier studies have found that over one-third of the nitrophenols and the majority of the dinitrophenols are contributed by secondary formation (Harrison et

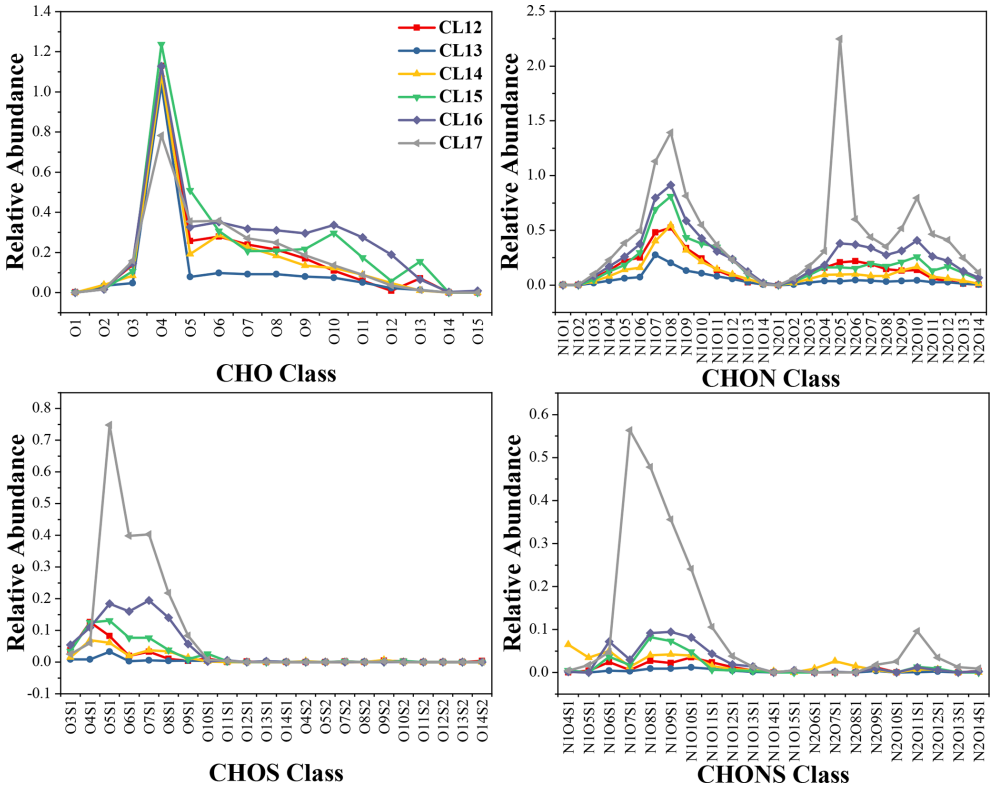

Figure 4. Relative abundance of the categories of CHO, CHON, CHOS, and CHONS formulas according to the characteristic atom groups within the molecular formulas in cloud water.

al., 2005). The transformation from 2-nitrophenol into 2,4-dinitrophenol was also observed during cloud events (Lüttke et al., 1997, 1999). Aqueous-phase radical nitration of mononitroaromatics has been reported to be a potential pathway to form dinitroaromatics (Lüttke et al., 1999; Kroflic et al., 2015; Cook et al., 2017). This implies that in-cloud aqueous-phase reactions represent the main formation pathway of dinitrophenols at the observation site.

Generally, CHON in cloud water has a higher f_{RA} during the nighttime (56.2 %–65.3 %) compared with the daytime (43.6 %–54.9 %; Table S2), which is consistent with the previous findings for aerosols (O'Brien et al., 2014). Particularly, the relative abundance of possible dinitrophenols formulas increases significantly at night. The representative formulas, including $C_6H_4N_2O_5$, $C_7H_6N_2O_5$, and $C_8H_8N_2O_5$, account for 0.5 %, 0.1 %, 0.4 %, 0.7 %, 2.1 %, and 14.8 % of CHON in f_{RA} for samples CL12–17, respectively. Previous studies have revealed the differences in atmospheric chemistry between day and night. The daytime chemistry is dominated by photochemical reactions in which OH• oxidation and photolysis represent the main processes in the aqueous phase (Ervens et al., 2011), while, during the nighttime, the NO_3• is dominant (Herrmann et al., 2010). The radical nitration of phenols by NO_2• and NO_3• leads to the formation of nitrophenols (Harrison et al., 2005). Thus, the high abundance of $-N_2O_5$ formulas may be attributed to the aqueous-phase formation of these possible dinitrophenols at night, while, during the daytime, the direct photolysis of nitrophenols would release NO_2^- and NO_3^- (Harrison et al., 2005; Chen et al., 2005; Bejan et al., 2006), causing the observed low relative abundance of dinitrophenols. A recent study conducted in the Field Museum at Tama Hill, Japan, observed that aerosol liquid water accelerated the formation of water-soluble organic nitrogen (WSON), especially at night, and the authors suggested that aqueous-phase reactions between NH_4^+ or reactive nitrogen and BVOCs at night contribute significantly to WSON in particles (Xu et al., 2020). In this study, the elevated abundance of N-containing organics in cloud water at night is mainly contributed by dinitrophenols and their derivatives, which are the products of radical nitration in the aqueous phase, indicating another possible pathway for the generation of WSON.

3.4.2 Formation of oxygenated organic matter and organosulfates

For CHO, the most abundant $C_{17}H_{26}O_4$ in cloud water was also detected in α-pinene ozonolysis SOA, as we discussed in Sect. 3.3. However, it was not detected in $PM_{2.5}$ in this study, indicating that it may mainly form through in-cloud aqueous-phase reactions. Interestingly, CHO formulas in $PM_{2.5}$ samples peak at O_8 (Fig. S5), which is significantly higher than

cloud water (Fig. 4). This is consistent with the higher OS_C values appearing in $PM_{2.5}$ samples. Some highly oxidized molecules (HOMs; O/C $\geq$ 0.6), e.g., $C_7H_{10}O_5$, $C_8H_{12}O_5$, and $C_{13}H_{24}O_{13}$, are identified in cloud water. However, the HOMs in cloud water only account for 12.6 %–32.2 % of the total CHO in terms of f_{RA}. A higher f_{RA} of CHO is observed during the daytime (Fig. 1b), which may result from the photochemical oxidation (e.g., the oxidation of volatile organic compounds; Ehn et al., 2014; Wang et al., 2017) and the photolysis of N- and S-containing formulas in cloud water under the illumination (Brüggemann et al., 2020; Laskin et al., 2015).

For CHOS formulas, the most abundant functions classes are similar between cloud water and $PM_{2.5}$. No statistical difference in the fraction of organosulfates is observed between cloud water and $PM_{2.5}$, except for a low f_{RA} (69.5 %) of organosulfates in the P2 sample, which may indicate the wide variety of formation mechanisms (e.g., acid-catalyzed particle-phase reactions and nucleophilic substitution reactions in aqueous phase) and/or other common sources of CHOS in cloud water and $PM_{2.5}$ (Brüggemann et al., 2020) but also the possible slightly enhanced formation of that in cloud water. S-containing formulas in cloud water are abundant at night (8.4 %–21.0 % in f_{RA}) compared with daytime (4.3 %–10.2 % in f_{RA}). We note that the f_{RA} of $CHOS_{O/S\geq4}$ at night (92.9 %–98.6 %) is slightly higher than that during the daytime (87.5 %–92.2 %). Thus, the formation of organosulfates likely enhances at night. In contrast, the photochemical oxidation of organosulfates results in the release of inorganic sulfate during the daytime, causing a low fraction of organosulfates.

4 Conclusions and atmospheric implications

This study investigated the molecular characteristics of cloud water using ESI FT-ICR MS and highlighted the crucial effects of in-cloud aqueous-phase reactions on the molecular composition and characteristics of cloud water. Thousands of formulas, including CHO, CHON, CHOS, and CHONS, were detected in which CHON and CHO formulas are dominant. Previous studies expected a higher oxidation state of organics in cloud water. However, no statistical difference between cloud water and $PM_{2.5}$ is observed in this study, while a higher OS_C of detected formulas, especially CHO, appears in $PM_{2.5}$ samples. Most formulas are identified as being aliphatic and olefinic species, and CHON and their aromatic structures are abundant in cloud water.

Our results showed that N-containing formulas are the most abundant in cloud water, which may be mainly related to the aqueous-phase formation. Dinitrophenols and their derivatives exist abundantly in cloud water, especially at night, suggesting the contribution of radical nitration on N-containing organics in cloud water. Meanwhile, organosulfates are also detected in cloud water, and a slightly higher fraction is observed at night, suggesting the dark-reaction formation. Nitroaromatic compounds have been identified as being one of the major light absorption components in brown carbon (X. Li et al., 2020) and are regarded as being the phytotoxin and suspected carcinogenic materials (Harrison et al., 2005). Organosulfates are thought to affect the physicochemical properties of aerosol, such as hygroscopicity and cloud condensation nuclei formation potential (Brüggemann et al., 2020). Thus, the aqueous-phase formation of N-containing organics and organosulfates at night are worth targeting. We noted that the database for the diurnal variation analysis is limited in this study, but the results provided novel insights into the diurnal variation in cloud chemistry. Firm conclusions warrant future field studies.

Data availability. The data set related to this work can be accessed via https://doi.org/10.5281/zenodo.5676489 (Sun, 2021).

Supplement. Supporting information includes one text (Text S1), five figures (Figs. S1–S5), and six tables (Tables S1–S6) related to the paper. The supplement related to this article is available online at: https://doi.org/10.5194/acp-21-16631-2021-supplement.

Author contributions. XB and GZ designed the research, with input from XW, PP, and GS. YF, FJ, and YY collected samples. WS and BJ carried out the sample pretreatment and instrumental analysis under the guidance of YL. WS processed data when YF and XL gave constructive discussion. WS wrote the paper, and XB, GZ and YF interpreted data and edited the paper. JC, DC, and JO had an active role in supporting the sampling work. All authors contributed to the discussions of the results and refinement of the paper.

Competing interests. The contact author has declared that neither they nor their co-authors have any competing interests

Disclaimer. Publisher's note: Copernicus Publications remains neutral with regard to jurisdictional claims in published maps and institutional affiliations.

Acknowledgements. The authors gratefully acknowledge Jianzhong Song and Chunlin Zou (Guangzhou Institute of Geochemistry, Chinese Academy of Sciences), for the guidance and assistance during sample pretreatment and for providing the raw data related to the article by Song et al. (2018), which is helpful to the discussion of this paper. This is contribution no. IS-3097 from GIGCAS.

Financial support. This research has been supported by the National Natural Science Foundation of China (grant nos. 41877307 and 42077322), the Natural Science Foundation of Guangdong

Province (grant no. 2019B151502022), and the Guangdong Foundation for Program of Science and Technology Research (grant nos. 2019B121202002 and 2019B121205006).

Review statement. This paper was edited by Sergey A. Nizkorodov and reviewed by three anonymous referees.

References

An, Y., Xu, J., Feng, L., Zhang, X., Liu, Y., Kang, S., Jiang, B., and Liao, Y.: Molecular characterization of organic aerosol in the Himalayas: insight from ultra-high-resolution mass spectrometry, Atmos. Chem. Phys., 19, 1115–1128, https://doi.org/10.5194/acp-19-1115-2019, 2019.

Bejan, I., Abd El Aal, Y., Barnes, I., Benter, T., Bohn, B., Wiesen, P., and Kleffmann, J.: The photolysis of ortho-nitrophenols: a new gas phase source of HONO, Phys. Chem. Chem. Phys., 8, 2028–2035, https://doi.org/10.1039/B516590C, 2006.

Bianco, A., Passananti, M., Deguillaume, L., Mailhot, G., and Brigante, M.: Tryptophan and tryptophan-like substances in cloud water: Occurrence and photochemical fate, Atmos. Environ., 137, 53–61, https://doi.org/10.1016/j.atmosenv.2016.04.034, 2016a.

Bianco, A., Voyard, G., Deguillaume, L., Mailhot, G., and Brigante, M.: Improving the characterization of dissolved organic carbon in cloud water: Amino acids and their impact on the oxidant capacity, Sci. Rep., 6, 37420, https://doi.org/10.1038/srep37420, 2016b.

Bianco, A., Deguillaume, L., Vaitilingom, M., Nicol, E., Baray, J. L., Chaumerliac, N., and Bridoux, M.: Molecular characterization of cloud water samples collected at the Puy de Dome (France) by Fourier Transform Ion Cyclotron Resonance Mass Spectrometry, Environ. Sci. Technol., 52, 10275–10285, https://doi.org/10.1021/acs.est.8b01964, 2018.

Bianco, A., Riva, M., Baray, J.-L., Ribeiro, M., Chaumerliac, N., George, C., Bridoux, M., and Deguillaume, L.: Chemical characterization of cloudwater collected at Puy de Dôme by FT-ICR MS reveals the presence of SOA components, ACS Earth Space Chem., 3, 2076–2087, https://doi.org/10.1021/acsearthspacechem.9b00153, 2019.

Blando, J. D. and Turpin, B. J.: Secondary organic aerosol formation in cloud and fog droplets: a literature evaluation of plausibility, Atmos. Environ., 34, 1623–1632, https://doi.org/10.1016/S1352-2310(99)00392-1, 2000.

Boone, E. J., Laskin, A., Laskin, J., Wirth, C., Shepson, P. B., Stirm, B. H., and Pratt, K. A.: Aqueous processing of atmospheric organic particles in cloud water collected via aircraft sampling, Environ. Sci. Technol., 49, 8523–8530, https://doi.org/10.1021/acs.est.5b01639, 2015.

Braman, T., Dolvin, L., Thrasher, C., Yu, H., Walhout, E. Q., and O'Brien, R. E.: Fresh versus photo-recalcitrant secondary organic aerosol: Effects of organic mixtures on aqueous photodegradation of 4-nitrophenol, Environ. Sci. Technol. Lett., 7, 248–253, https://doi.org/10.1021/acs.estlett.0c00177, 2020.

Brege, M., Paglione, M., Gilardoni, S., Decesari, S., Facchini, M. C., and Mazzoleni, L. R.: Molecular insights on aging and aqueous-phase processing from ambient biomass burning emissions-influenced Po Valley fog and aerosol, Atmos. Chem. Phys., 18, 13197–13214, https://doi.org/10.5194/acp-18-13197-2018, 2018.

Brüggemann, M., Xu, R., Tilgner, A., Kwong, K. C., Mutzel, A., Poon, H. Y., Otto, T., Schaefer, T., Poulain, L., Chan, M. N., and Herrmann, H.: Organosulfates in ambient aerosol: state of knowledge and future research directions on formation, abundance, fate, and importance, Environ. Sci. Technol., 54, 3767–3782, https://doi.org/10.1021/acs.est.9b06751, 2020.

Chen, B., Yang, C., and Goh, N. K.: Direct photolysis of nitroaromatic compounds in aqueous solutions, J. Environ. Sci. China, 17, 598–604, https://doi.org/10.1016/S1001-0742(06)60039-9, 2005.

Cho, Y., Ahmed, A., Islam, A., and Kim, S.: Developments in FT-ICR MS instrumentation, ionization techniques, and data interpretation methods for petroleomics, Mass. Spectrom. Rev., 34, 248–263, https://doi.org/10.1002/mas.21438, 2015.

Cook, R. D., Lin, Y.-H., Peng, Z., Boone, E., Chu, R. K., Dukett, J. E., Gunsch, M. J., Zhang, W., Tolic, N., Laskin, A., and Pratt, K. A.: Biogenic, urban, and wildfire influences on the molecular composition of dissolved organic compounds in cloud water, Atmos. Chem. Phys., 17, 15167–15180, https://doi.org/10.5194/acp-17-15167-2017, 2017.

Darer, A. I., Cole-Filipiak, N. C., O'Connor, A. E., and Elrod, M. J.: Formation and stability of atmospherically relevant isoprene-derived organosulfates and organonitrates, Environ. Sci. Technol., 45, 1895–1902, https://doi.org/10.1021/es103797z, 2011.

Deguillaume, L., Leriche, M., Desboeufs, K., Mailhot, G., George, C., and Chaumerliac, N.: Transition metals in atmospheric liquid phases: Sources, reactivity, and sensitive parameters, Chem. Rev., 105, 3388–3431, https://doi.org/10.1021/cr040649c, 2005.

De Haan, D. O., Corrigan, A. L., Smith, K. W., Stroik, D. R., Turley, J. J., Lee, F. E., Tolbert, M. A., Jimenez, J. L., Cordova, K. E., and Ferrell, G. R.: Secondary organic aerosol-forming reactions of glyoxal with amino acids, Environ. Sci. Technol., 43, 2818–2824, https://doi.org/10.1021/es803534f, 2009.

De Haan, D. O., Hawkins, L. N., Kononenko, J. A., Turley, J. J., Corrigan, A. L., Tolbert, M. A., and Jimenez, J. L.: Formation of nitrogen-containing oligomers by methylglyoxal and amines in simulated evaporating cloud droplets, Environ. Sci. Technol., 45, 984–991, https://doi.org/10.1021/es102933x, 2011.

De Haan, D. O., Tapavicza, E., Riva, M., Cui, T., Surratt, J. D., Smith, A. C., Jordan, M. C., Nilakantan, S., Almodovar, M., Stewart, T. N., de Loera, A., De Haan, A. C., Cazaunau, M., Gratien, A., Pangui, E., and Doussin, J. F.: Nitrogen-containing, light-absorbing oligomers produced in aerosol particles exposed to methylglyoxal, photolysis, and cloud cycling, Environ. Sci. Technol., 52, 4061–4071, https://doi.org/10.1021/acs.est.7b06105, 2018.

Demoz, B. B., Collett Jr., J. L., and Daube Jr., B. C.: On the caltech active strand cloudwater collectors, Atmos. Res., 41, 47–62, https://doi.org/10.1016/0169-8095(95)00044-5, 1996.

Ehn, M., Thornton, J. A., Kleist, E., Sipila, M., Junninen, H., Pullinen, I., Springer, M., Rubach, F., Tillmann, R., Lee, B., Lopez-Hilfiker, F., Andres, S., Acir, I. H., Rissanen, M., Jokinen, T., Schobesberger, S., Kangasluoma, J., Kontkanen, J., Nieminen, T., Kurten, T., Nielsen, L. B., Jorgensen, S., Kjaergaard, H. G., Canagaratna, M., Maso, M. D., Berndt, T., Petaja, T., Wahner, A., Kerminen, V. M., Kulmala, M., Worsnop,

D. R., Wildt, J., and Mentel, T. F.: A large source of low-volatility secondary organic aerosol, Nature, 506, 476–479, https://doi.org/10.1038/nature13032, 2014.

Ehrenhauser, F. S., Khadapkar, K., Wang, Y., Hutchings, J. W., Delhomme, O., Kommalapati, R. R., Herckes, P., Wornat, M. J., and Valsaraj, K. T.: Processing of atmospheric polycyclic aromatic hydrocarbons by fog in an urban environment, J. Environ. Monitor., 14, 2566–2579, https://doi.org/10.1039/c2em30336a, 2012.

Ervens, B., Turpin, B. J., and Weber, R. J.: Secondary organic aerosol formation in cloud droplets and aqueous particles (aqSOA): a review of laboratory, field and model studies, Atmos. Chem. Phys., 11, 11069–11102, https://doi.org/10.5194/acp-11-11069-2011, 2011.

Ervens, B., Wang, Y., Eagar, J., Leaitch, W. R., Macdonald, A. M., Valsaraj, K. T., and Herckes, P.: Dissolved organic carbon (DOC) and select aldehydes in cloud and fog water: the role of the aqueous phase in impacting trace gas budgets, Atmos. Chem. Phys., 13, 5117–5135, https://doi.org/10.5194/acp-13-5117-2013, 2013.

Feingold, G., Kreidenweis, S. M., and Zhang, Y. P.: Stratocumulus processing of gases and cloud condensation nuclei - 1, Trajectory ensemble model, J. Geophys. Res.-Atmos., 103, 19527–19542, https://doi.org/10.1029/98JD01750, 1998.

Ge, X., Zhang, Q., Sun, Y., Ruehl, C. R., and Setyan, A.: Effect of aqueous-phase processing on aerosol chemistry and size distributions in Fresno, California, during wintertime, Environ. Chem., 9, 221–235, https://doi.org/10.1071/en11168, 2012.

Guo, J., Wang, Y., Shen, X., Wang, Z., Lee, T., Wang, X., Li, P., Sun, M., Collett, J. L., Wang, W., and Wang, T.: Characterization of cloud water chemistry at Mount Tai, China: Seasonal variation, anthropogenic impact, and cloud processing, Atmos. Environ., 60, 467–476, https://doi.org/10.1016/j.atmosenv.2012.07.016, 2012.

Hallquist, M., Wenger, J. C., Baltensperger, U., Rudich, Y., Simpson, D., Claeys, M., Dommen, J., Donahue, N. M., George, C., Goldstein, A. H., Hamilton, J. F., Herrmann, H., Hoffmann, T., Iinuma, Y., Jang, M., Jenkin, M. E., Jimenez, J. L., Kiendler-Scharr, A., Maenhaut, W., McFiggans, G., Mentel, Th. F., Monod, A., Prévôt, A. S. H., Seinfeld, J. H., Surratt, J. D., Szmigielski, R., and Wildt, J.: The formation, properties and impact of secondary organic aerosol: current and emerging issues, Atmos. Chem. Phys., 9, 5155–5236, https://doi.org/10.5194/acp-9-5155-2009, 2009.

Harrison, M. A. J., Barra, S., Borghesi, D., Vione, D., Arsene, C., and Iulian Olariu, R.: Nitrated phenols in the atmosphere: a review, Atmos. Environ., 39, 231–248, https://doi.org/10.1016/j.atmosenv.2004.09.044, 2005.

Herckes, P., Hannigan, M. P., Trenary, L., Lee, T., and Collett Jr., J. L.: Organic compounds in radiation fogs in Davis (California), Atmos. Res., 64, 99–108, https://doi.org/10.1016/S0169-8095(02)00083-2, 2002.

Herckes, P., Valsaraj, K. T., and Collett, J. L.: A review of observations of organic matter in fogs and clouds: Origin, processing and fate, Atmos. Res., 132–133, 434–449, https://doi.org/10.1016/j.atmosres.2013.06.005, 2013.

Herrmann, H., Hoffmann, D., Schaefer, T., Brauer, P., and Tilgner, A.: Tropospheric aqueous-phase free-radical chemistry: radical sources, spectra, reaction kinetics and prediction tools, Chemphyschem, 11, 3796–3822, https://doi.org/10.1002/cphc.201000533, 2010.

Herrmann, H., Schaefer, T., Tilgner, A., Styler, S. A., Weller, C., Teich, M., and Otto, T.: Tropospheric aqueous-phase chemistry: kinetics, mechanisms, and its coupling to a changing gas phase, Chem. Rev., 115, 4259–4334, https://doi.org/10.1021/cr500447k, 2015.

Hockaday, W. C., Purcell, J. M., Marshall, A. G., Baldock, J. A., and Hatcher, P. G.: Electrospray and photoionization mass spectrometry for the characterization of organic matter in natural waters: a qualitative assessment, Limnol. Oceanogr.-Meth., 7, 81–95, https://doi.org/10.4319/lom.2009.7.81, 2009.

Huang, D. D., Zhang, Q., Cheung, H. H. Y., Yu, L., Zhou, S., Anastasio, C., Smith, J. D., and Chan, C. K.: Formation and evolution of aqSOA from aqueous-Phase reactions of phenolic carbonyls: Comparison between ammonium sulfate and ammonium nitrate solutions, Environ. Sci. Technol., 52, 9215–9224, https://doi.org/10.1021/acs.est.8b03441, 2018.

Jiang, B., Zhan, Z. W., Shi, Q., Liao, Y., Zou, Y. R., Tian, Y., and Peng, P.: Chemometric unmixing of petroleum mixtures by negative ion ESI FT-ICR MS analysis, Anal. Chem., 91, 2209–2215, https://doi.org/10.1021/acs.analchem.8b04790, 2019.

Kim, H., Collier, S., Ge, X., Xu, J., Sun, Y., Jiang, W., Wang, Y., Herckes, P., and Zhang, Q.: Chemical processing of water-soluble species and formation of secondary organic aerosol in fogs, Atmos. Environ., 200, 158–166, https://doi.org/10.1016/j.atmosenv.2018.11.062, 2019.

Koch, B. P. and Dittmar, T.: From mass to structure: an aromaticity index for high-resolution mass data of natural organic matter, Rapid Commun. Mass Sp., 20, 926–932, https://doi.org/10.1002/rcm.2386, 2006.

Kroflic, A., Grilc, M., and Grgic, I.: Does toxicity of aromatic pollutants increase under remote atmospheric conditions?, Sci. Rep., 5, 8859, https://doi.org/10.1038/srep08859, 2015.

Kroll, J. H., Donahue, N. M., Jimenez, J. L., Kessler, S. H., Canagaratna, M. R., Wilson, K. R., Altieri, K. E., Mazzoleni, L. R., Wozniak, A. S., Bluhm, H., Mysak, E. R., Smith, J. D., Kolb, C. E., and Worsnop, D. R.: Carbon oxidation state as a metric for describing the chemistry of atmospheric organic aerosol, Nat. Chem., 3, 133–139, https://doi.org/10.1038/nchem.948, 2011.

Kua, J., Krizner, H. E., and De Haan, D. O.: Thermodynamics and kinetics of imidazole formation from glyoxal, methylamine, and formaldehyde: a computational study, J. Phys. Chem. A, 115, 1667–1675, https://doi.org/10.1021/jp111527x, 2011.

Laskin, A., Laskin, J., and Nizkorodov, S. A.: Chemistry of atmospheric brown carbon, Chem. Rev., 115, 4335–4382, https://doi.org/10.1021/cr5006167, 2015.

Leclair, J. P., Collett, J. L., and Mazzoleni, L. R.: Fragmentation analysis of water-soluble atmospheric organic matter using ultrahigh-resolution FT-ICR mass spectrometry, Environ. Sci. Technol., 46, 4312–4322, https://doi.org/10.1021/es203509b, 2012.

Li, T., Wang, Z., Wang, Y., Wu, C., Liang, Y., Xia, M., Yu, C., Yun, H., Wang, W., Wang, Y., Guo, J., Herrmann, H., and Wang, T.: Chemical characteristics of cloud water and the impacts on aerosol properties at a subtropical mountain site in Hong Kong SAR, Atmos. Chem. Phys., 20, 391–407, https://doi.org/10.5194/acp-20-391-2020, 2020.

Li, X., Wang, Y., Hu, M., Tan, T., Li, M., Wu, Z., Chen, S., and Tang, X.: Characterizing chemical composition and light absorption of nitroaromatic compounds in the winter of Beijing, Atmos. Environ., 237, 117712, https://doi.org/10.1016/j.atmosenv.2020.117712, 2020.

Li, Y. J., Huang, D. D., Cheung, H. Y., Lee, A. K. Y., and Chan, C. K.: Aqueous-phase photochemical oxidation and direct photolysis of vanillin – a model compound of methoxy phenols from biomass burning, Atmos. Chem. Phys., 14, 2871–2885, https://doi.org/10.5194/acp-14-2871-2014, 2014.

Lin, P., Yu, J. Z., Engling, G., and Kalberer, M.: Organosulfates in humic-like substance fraction isolated from aerosols at seven locations in East Asia: a study by ultra-high-resolution mass spectrometry, Environ. Sci. Technol., 46, 13118–13127, https://doi.org/10.1021/es303570v, 2012.

Lin, Q., Zhang, G., Peng, L., Bi, X., Wang, X., Brechtel, F. J., Li, M., Chen, D., Peng, P., Sheng, G., and Zhou, Z.: In situ chemical composition measurement of individual cloud residue particles at a mountain site, southern China, Atmos. Chem. Phys., 17, 8473–8488, https://doi.org/10.5194/acp-17-8473-2017, 2017.

Löflund, M., Kasper-Giebl, A., Schuster, B., Giebl, H., Hitzenberger, R., and Puxbaum, H.: Formic, acetic, oxalic, malonic andsuccinic acid concentrations andtheir contribution to organic carbon in cloudwater, Atmos. Environ., 36, 1553–1558, https://doi.org/10.1016/S1352-2310(01)00573-8, 2002.

Lüttke, J., Scheer, V., Levsen, K., Wünsch, G., Cape, J. N., Hargreaves, K. J., Storeton-West, R. L., Acker, K., Wieprecht, W., and Jones, B.: Occurrence and formation of nitrated phenols in and out of cloud, Atmos. Environ., 31, 2637–2648, https://doi.org/10.1016/S1352-2310(96)00229-4, 1997.

Lüttke, J., Levsen, K., Acker, K., Wieprecht, W., and Möller, D.: Phenols and nitrated phenols in clouds at Mount Brocken, Int. J. Environ. An. Ch., 74, 69–89, https://doi.org/10.1080/03067319908031417, 1999.

Mazzoleni, L. R., Ehrmann, B. M., Shen, X., Marshall, A. G., and Collett Jr., J. L.: Water-Soluble atmospheric organic matter in fog: Exact masses and chemical formula identification by ultrahigh-resolution Fourier Transform Ion Cyclotron Resonance Mass Spectrometry, Environ. Sci. Technol., 44, 3690–3697, https://doi.org/10.1021/es903409k, 2010.

Mazzoleni, L. R., Saranjampour, P., Dalbec, M. M., Samburova, V., Hallar, A. G., Zielinska, B., Lowenthal, D. H., and Kohl, S.: Identification of water-soluble organic carbon in non-urban aerosols using ultrahigh-resolution FT-ICR mass spectrometry: organic anions, Environ. Chem., 9, 285, https://doi.org/10.1071/en11167, 2012.

McNeill, V. F.: Aqueous organic chemistry in the atmosphere: sources and chemical processing of organic aerosols, Environ. Sci. Technol., 49, 1237–1244, https://doi.org/10.1021/es5043707, 2015.

O'Brien, R. E., Laskin, A., Laskin, J., Rubitschun, C. L., Surratt, J. D., and Goldstein, A. H.: Molecular characterization of S- and N-containing organic constituents in ambient aerosols by negative ion mode high-resolution Nanospray Desorption Electrospray Ionization Mass Spectrometry: CalNex 2010 field study, J. Geophys. Res.-Atmos., 119, 12706–12720, https://doi.org/10.1002/2014jd021955, 2014.

Paglione, M., Gilardoni, S., Rinaldi, M., Decesari, S., Zanca, N., Sandrini, S., Giulianelli, L., Bacco, D., Ferrari, S., Poluzzi, V., Scotto, F., Trentini, A., Poulain, L., Herrmann, H., Wiedensohler, A., Canonaco, F., Prévôt, A. S. H., Massoli, P., Carbone, C., Facchini, M. C., and Fuzzi, S.: The impact of biomass burning and aqueous-phase processing on air quality: a multi-year source apportionment study in the Po Valley, Italy, Atmos. Chem. Phys., 20, 1233–1254, https://doi.org/10.5194/acp-20-1233-2020, 2020.

Park, J.-H., Babar, Z. B., Baek, S. J., Kim, H. S., and Lim, H.-J.: Effects of NO_x on the molecular composition of secondary organic aerosol formed by the ozonolysis and photooxidation of α-pinene, Atmos. Environ., 166, 263–275, https://doi.org/10.1016/j.atmosenv.2017.07.022, 2017.

Putman, A. L., Offenberg, J. H., Fisseha, R., Kundu, S., Rahn, T. A., and Mazzoleni, L. R.: Ultrahigh-resolution FT-ICR mass spectrometry characterization of α-pinene ozonolysis SOA, Atmos. Environ., 46, 164–172, https://doi.org/10.1016/j.atmosenv.2011.10.003, 2012.

Reed Harris, A. E., Ervens, B., Shoemaker, R. K., Kroll, J. A., Rapf, R. J., Griffith, E. C., Monod, A., and Vaida, V.: Photochemical kinetics of pyruvic acid in aqueous solution, J. Phys. Chem. A, 118, 8505–8516, https://doi.org/10.1021/jp502186q, 2014.

Renard, P., Siekmann, F., Salque, G., Demelas, C., Coulomb, B., Vassalo, L., Ravier, S., Temime-Roussel, B., Voisin, D., and Monod, A.: Aqueous-phase oligomerization of methyl vinyl ketone through photooxidation – Part 1: Aging processes of oligomers, Atmos. Chem. Phys., 15, 21–35, https://doi.org/10.5194/acp-15-21-2015, 2015.

Rudziński, K. J. and Szmigielski, R.: Aqueous reactions of sulfate radical-anions with nitrophenols in atmospheric context, Atmosphere, 10, 795–809, https://doi.org/10.3390/atmos10120795, 2019.

Sareen, N., Carlton, A. G., Surratt, J. D., Gold, A., Lee, B., Lopez-Hilfiker, F. D., Mohr, C., Thornton, J. A., Zhang, Z., Lim, Y. B., and Turpin, B. J.: Identifying precursors and aqueous organic aerosol formation pathways during the SOAS campaign, Atmos. Chem. Phys., 16, 14409–14420, https://doi.org/10.5194/acp-16-14409-2016, 2016.

Schurman, M. I., Boris, A., Desyaterik, Y., and Collett, J. L.: Aqueous secondary organic aerosol formation in ambient cloud water photo-oxidations, Aerosol Air Qual. Res., 18, 15–25, https://doi.org/10.4209/aaqr.2017.01.0029, 2018.

Sleighter, R. L., Liu, Z., Xue, J., and Hatcher, P. G.: Multivariate statistical approaches for the characterization of dissolved organic matter analyzed by ultrahigh resolution mass spectrometry, Environ. Sci. Technol., 44, 7576–7582, https://doi.org/10.1021/es1002204, 2010.

Smith, J. D., Sio, V., Yu, L., Zhang, Q., and Anastasio, C.: Secondary organic aerosol production from aqueous reactions of atmospheric phenols with an organic triplet excited state, Environ. Sci. Technol., 48, 1049–1057, https://doi.org/10.1021/es4045715, 2014.

Song, J., Li, M., Jiang, B., Wei, S., Fan, X., and Peng, P.: Molecular characterization of water-soluble humic like substances in smoke particles emitted from combustion of biomass materials and coal using ultrahigh-resolution Electrospray Ionization Fourier Transform Ion Cyclotron Resonance Mass Spectrometry, Environ. Sci. Technol., 52, 2575–2585, https://doi.org/10.1021/acs.est.7b06126, 2018.

Stein, A. F., Draxler, R. R., Rolph, G. D., Stunder, B. J. B., Cohen, M. D., and Ngan, F.: NOAA's HYSPLIT Atmospheric Transport and Dispersion Modeling System, B. Am. Meteorol. Soc., 96, 2059–2077, https://doi.org/10.1175/bams-d-14-00110.1, 2015.

Stevens, B., Feingold, G., Cotton, W. R., and Walko, R. L.: Elements of the microphysical structure of numerically simulated nonprecipitating stratocumulus, J. Atmos. Sci., 53, 980–1006, https://doi.org/10.1175/1520-0469(1996)053<0980:EOTMSO>2.0.CO;2, 1996.

Stubenrauch, C. J., Rossow, W. B., Kinne, S., Ackerman, S., Cesana, G., Chepfer, H., Di Girolamo, L., Getzewich, B., Guignard, A., Heidinger, A., Maddux, B. C., Menzel, W. P., Minnis, P., Pearl, C., Platnick, S., Poulsen, C., Riedi, J., Sun-Mack, S., Walther, A., Winker, D., Zeng, S., and Zhao, G.: Assessment of global cloud datasets from satellites: project and database initiated by the GEWEX radiation panel, B. Am. Meteorol. Soc., 94, 1031–1049, https://doi.org/10.1175/bams-d-12-00117.1, 2013.

Sun, X., Wang, Y., Li, H., Yang, X., Sun, L., Wang, X., Wang, T., and Wang, W.: Organic acids in cloud water and rainwater at a mountain site in acid rain areas of South China, Environ. Sci. Pollut. Res. Int., 23, 9529–9539, https://doi.org/10.1007/s11356-016-6038-1, 2016.

Sun, Y. L., Zhang, Q., Anastasio, C., and Sun, J.: Insights into secondary organic aerosol formed via aqueous-phase reactions of phenolic compounds based on high resolution mass spectrometry, Atmos. Chem. Phys., 10, 4809–4822, https://doi.org/10.5194/acp-10-4809-2010, 2010.

Sun, W.: Dataset for article "Measurement report: Molecular characteristics of cloud water in southern China and insights into aqueous-phase processes from Fourier Transform Ion Cyclotron Resonance Mass Spectrometry", Zenodo [data set], https://doi.org/10.5281/zenodo.5676489, 2021.

Szmigielski, R.: Evidence for C5 organosulfur secondary organic aerosol components from in-cloud processing of isoprene: Role of reactive SO4 and SO3 radicals, Atmos. Environ., 130, 14–22, https://doi.org/10.1016/j.atmosenv.2015.10.072, 2016.

Tang, J., Li, J., Su, T., Han, Y., Mo, Y., Jiang, H., Cui, M., Jiang, B., Chen, Y., Tang, J., Song, J., Peng, P., and Zhang, G.: Molecular compositions and optical properties of dissolved brown carbon in biomass burning, coal combustion, and vehicle emission aerosols illuminated by excitation–emission matrix spectroscopy and Fourier transform ion cyclotron resonance mass spectrometry analysis, Atmos. Chem. Phys., 20, 2513–2532, https://doi.org/10.5194/acp-20-2513-2020, 2020.

van Pinxteren, D., Fomba, K. W., Mertes, S., Müller, K., Spindler, G., Schneider, J., Lee, T., Collett, J. L., and Herrmann, H.: Cloud water composition during HCCT-2010: Scavenging efficiencies, solute concentrations, and droplet size dependence of inorganic ions and dissolved organic carbon, Atmos. Chem. Phys., 16, 3185–3205, https://doi.org/10.5194/acp-16-3185-2016, 2016.

Wang, D., Li, Y., Yang, M., and Han, M.: Decomposition of polycyclic aromatic hydrocarbons in atmospheric aqueous droplets through sulfate anion radicals: an experimental and theoretical study, Sci. Total. Environ., 393, 64–71, https://doi.org/10.1016/j.scitotenv.2007.11.036, 2008.

Wang, J., Ye, J., Zhang, Q., Zhao, J., Wu, Y., Li, J., Liu, D., Li, W., Zhang, Y., Wu, C., Xie, C., Qin, Y., Lei, Y., Huang, X., Guo, J., Liu, P., Fu, P., Li, Y., Lee, H. C., Choi, H., Zhang, J., Liao, H., Chen, M., Sun, Y., Ge, X., Martin, S. T., and Jacob, D. J.: Aqueous production of secondary organic aerosol from fossil-fuel emissions in winter Beijing haze, P. Natl. Acad. Sci. USA, 118, https://doi.org/10.1073/pnas.2022179118, 2021.

Wang, M., Perroux, H., Fleuret, J., Bianco, A., Bouvier, L., Colomb, A., Borbon, A., and Deguillaume, L.: Anthropogenic and biogenic hydrophobic VOCs detected in clouds at the puy de Dôme station using Stir Bar Sorptive Extraction: Deviation from the Henry's law prediction, Atmos. Res., 237, 104844, https://doi.org/10.1016/j.atmosres.2020.104844, 2020.

Wang, S., Wu, R., Berndt, T., Ehn, M., and Wang, L.: Formation of highly oxidized radicals and multifunctional products from the atmospheric oxidation of alkylbenzenes, Environ. Sci. Technol., 51, 8442–8449, https://doi.org/10.1021/acs.est.7b02374, 2017.

Wozniak, A. S., Willoughby, A. S., Gurganus, S. C., and Hatcher, P. G.: Distinguishing molecular characteristics of aerosol water soluble organic matter from the 2011 trans-North Atlantic US GEOTRACES cruise, Atmos. Chem. Phys., 14, 8419–8434, https://doi.org/10.5194/acp-14-8419-2014, 2014.

Xu, Y., Miyazaki, Y., Tachibana, E., Sato, K., Ramasamy, S., Mochizuki, T., Sadanaga, Y., Nakashima, Y., Sakamoto, Y., Matsuda, K., and Kajii, Y.: Aerosol liquid water promotes the formation of water-soluble organic nitrogen in submicrometer aerosols in a suburban forest, Environ. Sci. Technol., 54, 1406–1414, https://doi.org/10.1021/acs.est.9b05849, 2020.

Ye, Z., Zhuang, Y., Chen, Y., Zhao, Z., Ma, S., Huang, H., Chen, Y., and Ge, X.: Aqueous-phase oxidation of three phenolic compounds by hydroxyl radical: Insight into secondary organic aerosol formation yields, mechanisms, products and optical properties, Atmos. Environ., 223, 117240, https://doi.org/10.1016/j.atmosenv.2019.117240, 2020.

Yu, L., Smith, J., Laskin, A., George, K. M., Anastasio, C., Laskin, J., Dillner, A. M., and Zhang, Q.: Molecular transformations of phenolic SOA during photochemical aging in the aqueous phase: competition among oligomerization, functionalization, and fragmentation, Atmos. Chem. Phys., 16, 4511–4527, https://doi.org/10.5194/acp-16-4511-2016, 2016.

Zhang, H., Yee, L. D., Lee, B. H., Curtis, M. P., Worton, D. R., Isaacman-VanWertz, G., Offenberg, J. H., Lewandowski, M., Kleindienst, T. E., Beaver, M. R., Holder, A. L., Lonneman, W. A., Docherty, K. S., Jaoui, M., Pye, H. O. T., Hu, W., Day, D. A., Campuzano-Jost, P., Jimenez, J. L., Guo, H., Weber, R. J., de Gouw, J., Koss, A. R., Edgerton, E. S., Brune, W., Mohr, C., Lopez-Hilfiker, F. D., Lutz, A., Kreisberg, N. M., Spielman, S. R., Hering, S. V., Wilson, K. R., Thornton, J. A., and Goldstein, A. H.: Monoterpenes are the largest source of summertime organic aerosol in the southeastern United States, P. Natl. Acad. Sci. USA, 115, 2038–2043, https://doi.org/10.1073/pnas.1717513115, 2018.

Zhao, Y., Hallar, A. G., and Mazzoleni, L. R.: Atmospheric organic matter in clouds: exact masses and molecular formula identification using ultrahigh-resolution FT-ICR mass spectrometry, Atmos. Chem. Phys., 13, 12343–12362, https://doi.org/10.5194/acp-13-12343-2013, 2013.

Zou, C., Li, M., Cao, T., Zhu, M., Fan, X., Peng, S., Song, J., Jiang, B., Jia, W., Yu, C., Song, H., Yu, Z., Li, J., Zhang, G., and Peng, P. a.: Comparison of solid phase extraction methods for the measurement of humic-like substances (HULIS) in atmospheric particles, Atmos. Environ., 225, 117370, https://doi.org/10.1016/j.atmosenv.2020.117370, 2020.